

Probing the mechanism of simultaneous two-electron emission on core-hole decay

Y. Hikosaka,¹ P. Lablanquie,^{2,3} F. Penent,^{2,3} P. Selles,^{2,3} T. Kaneyasu,¹ E. Shigemasa,¹ J. H. D. Eland,⁴ and K. Ito⁵

¹UVSOR Facility, Institute for Molecular Science, Okazaki 444-8585, Japan

²UPMC, Université Paris 06, LCPMR, 11 rue Pierre et Marie Curie, 75231 Paris Cedex 05, France

³CNRS, LCPMR (UMR 7614), 11 rue Pierre et Marie Curie, 75231 Paris Cedex 05, France

⁴Physical and Theoretical Chemistry Laboratory, South Parks Road, Oxford OX1 3QZ, United Kingdom

⁵Photon Factory, Institute of Materials Structure Science, Oho, Tsukuba 305-0801, Japan

(Received 11 May 2009; published 21 September 2009)

Simultaneous two-electron emission upon $2p$ core-electron excitation in Ar has been studied using a state-of-the-art multielectron coincidence method. Simultaneous two-electron emission effectively populates Rydberg-excited Ar^{2+} states, in which the excited electron behaves as a spectator of the direct double Auger decay of the core hole. This observation constitutes experimental evidence that the shake-off mechanism is not sufficient to model direct double Auger decay of a $2p$ hole in Ar and suggests an important contribution from the knock-out mechanism.

DOI: [10.1103/PhysRevA.80.031404](https://doi.org/10.1103/PhysRevA.80.031404)

PACS number(s): 32.80.Fb, 32.80.Hd, 32.80.Rm

The emission of two or more electrons from an atom after absorption of a single photon involves the many-body Coulomb interaction whose understanding is one of the unsolved fundamental problems in atomic and molecular physics. Double Auger (DA) decay of core-hole states and double photoionization (DPI) both lead to such two-electron emission. In both cases, two-electron emission may occur either as two successive steps or as a single simultaneous process. In the stepwise process the many-body problem can be simplified by considering each step individually. Particular interest is attached to the simultaneous process as it may require direct correlation between the motions of the electrons.

The mechanism generally invoked for simultaneous two-electron emission is “shake-off” [1,2]. In this purely quantum mechanical effect [3], the second electron ejection is the result of relaxation following the sudden change in central potential on ejection of the first electron. While this mechanism is a useful model of DA decay and DPI, theoretical calculations based entirely upon it often fail to match experimental cross sections and angular correlations between the two electrons. This disagreement has induced the development of theoretical approaches including electron correlation more explicitly [4–7]. In some theoretical frameworks, the introduction of the knock-out mechanism [8,9] in which a primary outgoing electron knocks out a second electron has noticeably improved agreement of the calculations with experiments [4,5]. However, so far no experiment has directly tested the inadequacy of the shake-off model.

In this Rapid Communication we show that the mechanism of simultaneous two-electron ejection in DA decay of core-hole states can be probed experimentally by prelocating a weakly bound electron by initial photoexcitation of a core electron to a Rydberg orbital. The retention or removal of the excited electron on direct DA decay of the core-hole gives key information about the mechanism. In practice, the experiment is to study resonant double Auger (RDA) decay of the core-excited state. Direct DA decay of the Ar $2p$ core-hole, which plays a benchmark role in the study of DA decay [7,10], shows a much larger probability than is calculated by considering the shake-off mechanism only [11]. In the present Rapid Communication we have investigated direct RDA processes in Ar $2p$ -electron to Rydberg-electron ex-

cited states. We have found notable spectator behavior of the Rydberg electron in the simultaneous release of two Auger electrons from the valence orbitals. Because the sudden change in central potential due to primary-valence-electron ejection should be more serious for a weakly bounded Rydberg electron than for another valence electron, retention of the Rydberg electron strongly suggests that the relaxation effect due to the primary ejection is not always enough to induce the ejection of the second valence electron. It is inferred that the shake-off model alone is not sufficient to describe the DA decay of the Ar $2p$ hole.

Experiments were performed at the undulator beamline BL-16A of the Photon Factory. Single-bunch operation of the storage ring provides a 624 ns repetition period for the 200-ps-width light pulses. Synchrotron radiation is monochromatized by a grazing-incidence monochromator using a varied-line-spacing plane grating, and the photon bandwidth was set at 30 meV. A mechanical chopper consisting in a cylinder rotating at 800 Hz with 100 slots (80 μm width) was employed to reduce the light pulse repetition rate by selecting one light pulse in every 12.5 μs [12]. Multiple coincidences were recorded between electrons analyzed in energy by their times of flight in a magnetic bottle electron spectrometer [13]. The descriptions of the analyzer and the data accumulation scheme are given elsewhere [12,14]. Conversion of the electron time of flight to energy was calibrated by measuring He photoelectron lines at different photon energies. The energy-resolving power of the apparatus, $E/\Delta E$, was estimated to be nearly constant at 60 for electrons of $E > 1$ eV, though ΔE was limited to around 20 meV [full width at half maximum (FWHM)] for $E < 1$ eV. The detection efficiency was constant around 60% for electrons of less than 200 eV [15].

Multiple electron coincidence data sets for Ar were accumulated at the five lower-lying $2p$ -to-Rydberg excited states indicated in the inset of Fig. 1. In addition, reference data sets have been obtained below (199.5 eV) and above (300.9 eV) the resonance range. Figure 1 shows histograms of the kinetic energy sum of the two electrons in coincidence, plotted as a function of Ar^{2+} binding energy. The contribution from valence DPI can be estimated to be at most 10% in the RDA decay yields on each resonance [16] and should exhibit

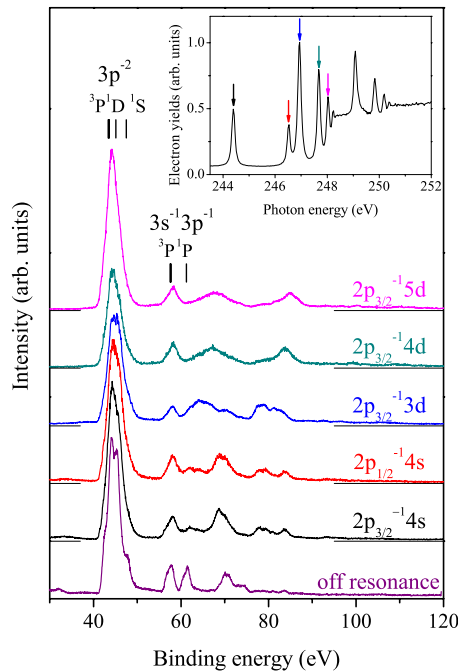


FIG. 1. (Color online) Spectra displaying the Ar^{2+} states populated via RDA decay of $2p$ -electron to Rydberg-electron states in Ar, as well via DPI at a photon energy of 199.5 eV. They are histograms of the kinetic energy sums for the two electrons detected in coincidence. The intensity of the spectrum measured at each resonance is normalized to the total electron yields included in the corresponding data set. The inset shows the total electron yield curve. The histograms correspond to increasing photon energies from bottom to top.

the same spectral shape as measured off resonance (bottom histogram). The predominant $\text{Ar}^{2+} 3p^{-2}$ and less favored $\text{Ar}^{2+} 3s^{-1}3p^{-1}$ formation are common to all the histograms obtained on the resonance states. In addition, formation of highly excited Ar^{2+} states is discernible in the binding energy range from 65 to 110 eV. The identities of the highly excited Ar^{2+} states formed are different for different initial Rydberg excitations, but the same Ar^{2+} states are populated after excitation to $4s$ from the $2p_{3/2}$ and $2p_{1/2}$ orbitals.

The experimental information on energy distributions between the two Auger electrons enables us to identify all RDA pathways and to extract information on the simultaneous two-electron emission process. Figure 2 displays the energy correlation map for the two Auger electrons emitted from the $\text{Ar} 2p_{3/2}^{-1}4s$ state, where intensity in the area corresponding to $E_s > E_f \times 0.2$ has been magnified by a factor of 30. Here, E_s and E_f are the energies of slow and fast Auger electrons, respectively. In this plot, coincidence counts associated with the formation of an individual Ar^{2+} state necessarily fall on a diagonal line defined by $E_f + E_s = (\text{photon energy}) - (\text{binding energy of the } \text{Ar}^{2+} \text{ state})$. Along the diagonal lines corresponding to $\text{Ar}^{2+} 3p^{-2}$ and $3s^{-1}3p^{-1}$ formation, intense spots are observed in the range of $E_f = 180\text{--}200$ eV. These spots result from cascade RDA processes, in which both electrons have discrete kinetic energies. On the other hand, the magnified area of the energy correlation map exhibits several diagonal stripes on which no clear spot structure due to cascade RDA process is present. These stripes

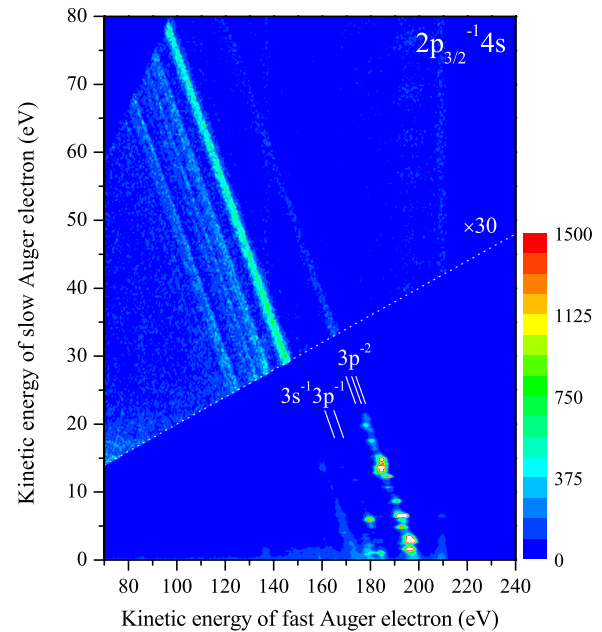


FIG. 2. (Color online) Energy correlation map for two Auger electrons emitted from the $\text{Ar} 2p_{3/2}^{-1}4s$ state lying at a photon energy of 244.39 eV, where the area of (slow electron energy) $>$ (fast electron energy) $\times 0.2$ is magnified by a factor of 30.

originate from direct RDA decay in which the two Auger electrons share the available energy continuously. We estimate that direct RDA processes contribute at most 30% to the total RDA decay yield at each core-excited state.

Figure 3(a) shows the intensity distribution on E_s along the diagonal line for the formation of $\text{Ar}^{2+} 3p^{-2}$ states. The peaks seen below 20 eV are assigned as autoionization from excited Ar^+ states of the $(3s, 3p)^{-2}4s$ configuration [17–19].

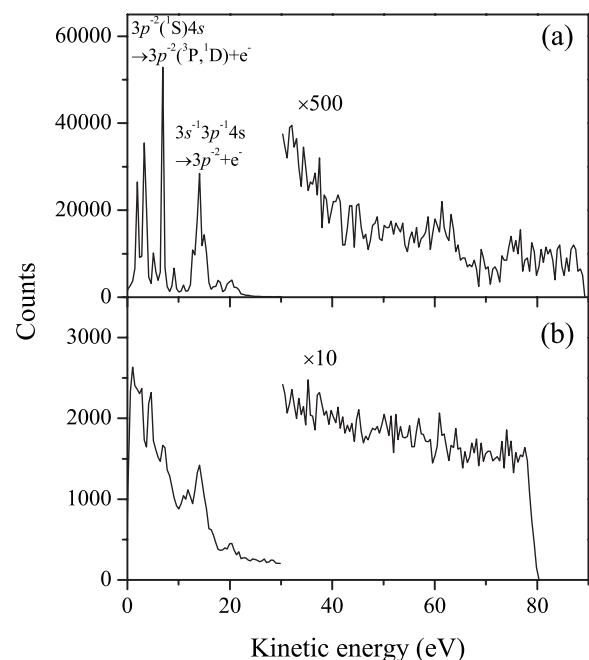


FIG. 3. Intensity distributions along diagonal stripes in Fig. 2: (a) formation of $\text{Ar}^{2+} 3p^{-2}$ and (b) formation of the Rydberg Ar^{2+} states around a binding energy of 70 eV.

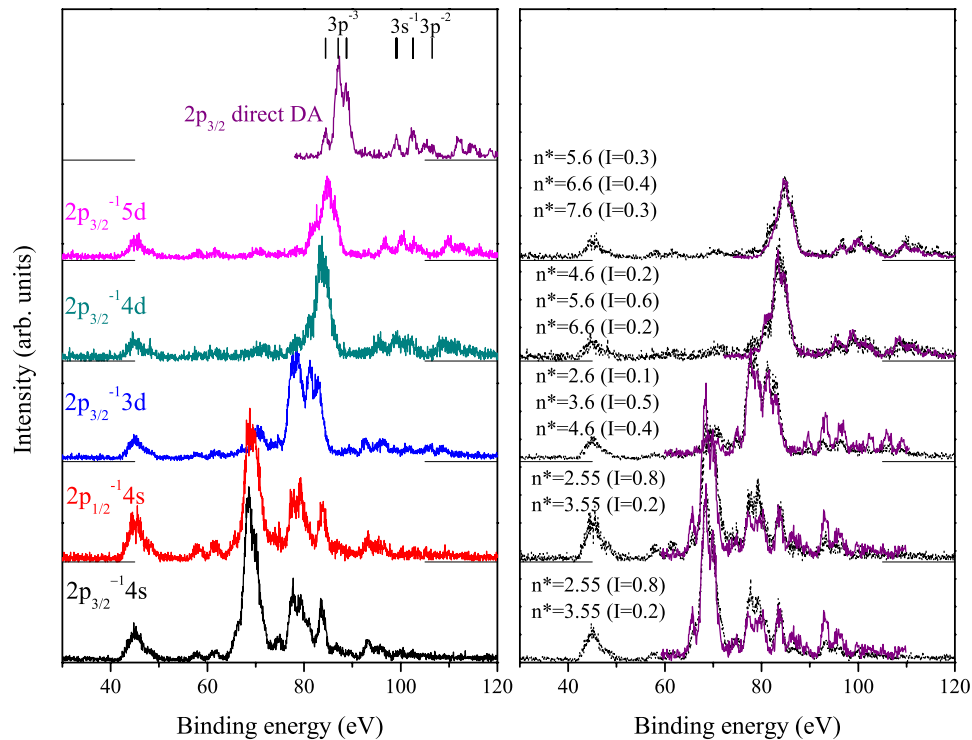


FIG. 4. (Color online) (Left) Spectra displaying the Ar^{2+} states populated via direct RDA decay, deduced as coincidence yields in the range of (slow electron energy) > (fast electron energy) $\times 0.2$. The intensity of each spectrum is normalized to the total electron yield included in the corresponding data set. The top spectrum shows the Ar^{3+} states populated by direct DA decay of the core-ionized $\text{Ar}^+ 2p_{3/2}^{-1}$ state. The spectrum is obtained from the coincidence data set accumulated at a photon energy of 300.9 eV, where energies of the slower electrons are restricted to >30 eV, in order to remove the indirect DA contribution [25]. (Right) Replots (dotted line) of the spectra in the left panel and fits (solid lines) using the spectral shape of direct DA decay. Two or three term values, whose nominal principal quantum number n^* are indicated, are included in the fitting. The relative intensity I of each term-value state is given in parenthesis.

These Ar^+ states lying above the Ar^{2+} threshold are populated by single Auger decay in which the initially excited Rydberg electron remains a spectator. Such cascade RDA processes make the predominant contribution to the $\text{Ar}^{2+} 3p^{-2}$ and $3s^{-1}3p^{-1}$ formation. By contrast, cascade RDA decay processes are relatively less significant in the formation of the highly excited Ar^{2+} states as can be seen in the corresponding intensity distribution shown in Fig. 3(b). Figure 3 also shows the continuous backgrounds corresponding to direct RDA decay. The background distributions in both curves show a gradual increase at decreasing kinetic energy and extend beneath the cascade RDA peaks. The increase is steeper in $\text{Ar}^{2+} 3p^{-2}$ formation than in the high-lying Ar^{2+} state formation.

To focus attention on Ar^{2+} states populated via direct RDA decay, a histogram of $E_f + E_s$ has been obtained for coincidence yields in the magnified area ($E_s > E_f \times 0.2$) of Fig. 2, thus effectively masking the contribution from the intense cascade RDA processes. The histogram obtained is plotted in the left panel of Fig. 4, together with those extracted in the same way on the other resonances, whose correlation maps show the same lack of cascade RDA processes in the corresponding areas. Each histogram shows strong formation of high-lying Ar^{2+} states and only weak $\text{Ar}^{2+} 3p^{-2}$ and $3s^{-1}3p^{-1}$ state formation. We have to keep in mind that these histograms exhibit the contributions from only a part of the whole RDA decay (where $E_s > E_f \times 0.2$) and do not re-

fect the whole Ar^{2+} populations via direct RDA decay; it can be expected that the $3p^{-2}$ states would be relatively more populated via direct RDA decay if we included the whole energy distributions which rise steeply down to 0 eV.

In Fig. 4, the manifold of high-lying Ar^{2+} states gradually shifts to higher binding energy as the initial core excitation is increased and becomes similar in structure to the Ar^{3+} states populated by direct DA decay of the core-ionized $\text{Ar}^+ 2p_{3/2}^{-1}$ state (top histogram). The high-lying Ar^{2+} states are, therefore, Rydberg states converging to Ar^{3+} states. In practice, the high-lying Ar^{2+} structures can be faithfully reproduced by using the spectral shape of the direct DA decay, where two or three term values are assumed in the fitting of each histogram (see the right panel of Fig. 4). As in most spectator processes of single Auger decay, promotions of the Rydberg electrons due to the change in the core ion charge can be identified. The promotion is stronger on RDA decay of higher core-excited states: an increase of 3 in effective principal quantum number has to be considered to reproduce the histograms for $\text{Ar} 2p_{3/2}^{-1}4d$ and $\text{Ar} 2p_{3/2}^{-1}5d$. The promotion distributions deduced shift slightly to higher final Rydberg orbitals, as compared with those in the single Auger decay [17], due to the stronger change in the core charge. A calculation with a simple hydrogenic model confirms the observed promotions in the RDA decay of the nd states [20], while it is also found that the RDA decay of the 4s states are beyond the range of adequacy of this simple model.

Direct RDA decay is sometimes called “Auger shake-off” [21]. This nomenclature is prompted by the assertion that direct RDA decay is the upper limit of the formation of shake-up Ar^+ states produced on single Auger decay. In this RDA process the Rydberg electron is shaken-off following single-Auger-electron emission and Ar^{2+} states with two valence holes are formed. Such a RDA process may contribute to the weak $\text{Ar}^{2+} 3p^{-2}$ and $3s^{-1}3p^{-1}$ formation seen in Fig. 4 although valence DPI contribution should be also sizable. The strong formation of Rydberg Ar^{2+} states found in the present observations shows that a considerable fraction of direct RDA decay has a different origin. The formation of these Rydberg Ar^{2+} states is most naturally attributed to non-involvement of the initial Rydberg electron in the direct RDA process, that is, the Rydberg electron behaves as a spectator of two electron ejections from the ion core. Therefore, direct RDA decay forming Rydberg Ar^{2+} states results from the nature of direct DA decay of the core hole.

We discuss next the mechanism of direct DA decay of the core hole, starting with the idea that its origin is pure shake-off. In this framework, the sudden change in the central potential on the primary valence-electron ejection leads to the secondary valence-electron ejection. But the removal of screening by the primary ejected electron has more effect on a Rydberg electron than on another valence electron [22]. In addition, the Rydberg electron is already closer to the electronic continuum than any valence electron. Therefore it is expected that in DA decay a pure shake-off mechanism, Rydberg electrons will be easily removed and formation of Rydberg Ar^{2+} states will be unlikely. However, in practice the Rydberg electron is not ejected but is only slightly promoted on DA decay of the core hole. The striking contrast between this expectation and the present observations demonstrates that the direct DA decay of the core hole cannot be fully attributed to the shake-off mechanism.

In response to the failure of the shake-off mechanism, we consider electron correlations through the knock-out mechanism. Here direct Coulomb interaction (inelastic collision) of the first Auger electron with another electron results in the ejection of a second electron. Interaction with another va-

lence electron must be much more probable than interaction with the distant Rydberg electron. It follows that the simultaneous ejection of two valence electrons, leaving the Rydberg electron in place, is the dominant predicted result for the knock-out mechanism. This mechanism therefore explains the observed formation of Rydberg Ar^{2+} states; the present observations demonstrate that it must make an important contribution to the overall DA decay.

These arguments are supported by the shape of the direct RDA distributions in Fig. 3. It is well established in DPI that the knock-out mechanism generally contributes well filled distributions of this sort, in contrast to the U-shape distributions expected from shake-off [4]. The relatively flat distribution in Fig. 3(b) is in agreement with the existence of an important contribution from the knock-out mechanism in the Rydberg Ar^{2+} formation, and the distribution in Fig. 3(a) indicates a dominant shake-off contribution for the $\text{Ar} 3p^{-2}$ formation.

In conclusion, RDA decay of core-excited states in Ar has been investigated using a state-of-the-art multiple coincidence method. We have found that Rydberg Ar^{2+} states are formed as an important product in direct RDA decay. The addition of a weakly bound Rydberg electron to the core-ionized states in the initial photoexcitation step has enabled us to probe the decay mechanism of the core hole. We have recorded similar observations of RDA decay in Ne, N_2 , and CO. These investigations also show predominant retention of Rydberg electrons in direct RDA decay. Observation of the same phenomenon for a range of targets proves experimentally that the shake-off mechanism alone is not sufficient to describe the direct DA decay of core holes in general. It is in accord with theoretical proposals of the limitation of the shake-off model in DA decay [6,11,23,24].

We are grateful to the Photon Factory staff for the stable operation of the PF ring. Financial support from JSPS and CNRS are acknowledged. J.H.D.E. thanks the Leverhulme Trust for support. This work was performed with the approval of the Photon Factory Advisory Committee (Proposal nos. 2006G230 and 2008G519).

-
- [1] T. Åberg, *Phys. Rev.* **156**, 35 (1967).
 [2] T. Pattard, T. Schneider, and J. M. Rost, *J. Phys. B* **36**, L189 (2003).
 [3] J. Colgan and M. S. Pindzola, *J. Phys. B* **37**, 1153 (2004).
 [4] T. Schneider, P. L. Chocian, and J.-M. Rost, *Phys. Rev. Lett.* **89**, 073002 (2002).
 [5] L. Avaldi and A. Huetz, *J. Phys. B* **38**, S861 (2005).
 [6] M. Y. Amusia, I. S. Lee, and V. A. Kilin, *Phys. Rev. A* **45**, 4576 (1992).
 [7] A. N. Grum-Grzhimailo and N. M. Kabachnik, *J. Phys. B* **37**, 1879 (2004).
 [8] J. A. R. Samson, *Phys. Rev. Lett.* **65**, 2861 (1990).
 [9] T. Pattard and J. Burgdörfer, *Phys. Rev. A* **64**, 042720 (2001).
 [10] J. Viehhaus *et al.*, *Phys. Rev. Lett.* **92**, 083001 (2004).
 [11] T. A. Carlson and M. O. Krause, *Phys. Rev. Lett.* **17**, 1079 (1966).
 [12] K. Ito *et al.* (unpublished).
 [13] J. H. D. Eland *et al.*, *Phys. Rev. Lett.* **90**, 053003 (2003).
 [14] Y. Hikosaka *et al.*, *Phys. Rev. Lett.* **97**, 053003 (2006).
 [15] T. Kaneyasu *et al.*, *Phys. Rev. A* **76**, 012717 (2007).
 [16] J. A. R. Samson, W. C. Stolte, Z. X. He, J. N. Cutler, and D. Hansen, *Phys. Rev. A* **54**, 2099 (1996).
 [17] J. Mursu *et al.*, *J. Phys. B* **29**, 4387 (1996).
 [18] S.-M. Huttula *et al.*, *J. Phys. B* **34**, 2325 (2001).
 [19] S.-M. Huttula *et al.*, *Phys. Rev. A* **63**, 032703 (2001).
 [20] P. Selles *et al.* (unpublished).
 [21] U. Becker *et al.*, *J. Phys. B* **22**, 749 (1989).
 [22] A. Kupliauskiene and K. Glemza, *J. Phys. B* **35**, 4637 (2002).
 [23] B. Kanngießner *et al.*, *Phys. Rev. A* **62**, 014702 (2000).
 [24] A. G. Kochur, V. L. Sukhorokov, and V. F. Demekhin, *J. Electron Spectrosc. Relat. Phenom.* **137-140**, 325 (2004).
 [25] P. Lablanquie *et al.*, *J. Electron Spectrosc. Relat. Phenom.* **156-158**, 51 (2007).